Numerical Simulation of Multi-Liquid Impinging Jets Using Volume of Fluid Method

Shakir Hussain Chaudhry, Khalid Parvez

Abstract— Liquid propellant rocket engines are an important part of space program. To achieve optimum performance and stability in case of liquid propelled rocket engines, good atomization and mixing characteristics of the fuel and oxidant are required. Injector element design based on impinging jet phenomenon for mixing and atomization are the ideal choice for engines using storable liquid propellants. This is due to their simple fabrication, good spray and mixing characteristics. In this paper, CFD technique was applied to numerically investigate the flow characteristics of impingement process of two liquid jets using Volume of Fluid (VOF) method with appropriate surface tension modeling for capturing liquid/gas interfaces. Different meshing techniques such as structured meshing with Adaptive Mesh Refinement and Coarsening were employed to efficiently capture the flows areas containing liquid/gas interfaces. Simulations results were compared with experimental results which are available in literature and flow patterns formed by liquid sheet breakup are also studied by comparing it with the experimental results.

Index Terms— Impinging Jets, Volume of Fluid (VOF), CFD, Atomization, Multi-Phase Flows

1 INTRODUCTION

Most of the atomizers used in propulsion, chemical engineering systems and material processing uses collision between two cylindrical liquid jets as a canonical configuration (Lefebvre 1989). Within a short distance from injection, flows which uses dynamic head of the liquid jet to disrupt the opposing stream usually use liquid impinging jet phenomena for atomization and mixing. Due to the effect of aerodynamic, surface tension and viscous forces the resultant sheet destabilizes and brakes into droplet. However atomization and mixing characteristics can also be enhanced by having a detailed understanding of different flow properties and then defining the configuration of injector geometry based on this study.

Most of the work that has been carried out in the field of Liquid Jet Impinging atomization is of experimental type and the literature is saturated with experimental results of liquid impinging jets. However, even then experimental results lack the details needed to fully understand the processes involved in the mixing and atomization. This lack of knowledge is due to the limitations of apparatus used to perform these experiments.

Most of the experimental studies carried out on impinging jet systems are used to develop relation of mean drop size and efficiency correlations for cold flow measurement. Work that shows important physical processes such as sheet breakup and drop size formation are less numerous. Hiedmann er al [1] carried out wide range of experimental study on atomization characteristics of turbulent impinging jets as function of pre-impingement length lj, length-to-diameter ratio L/do and orifice diameter do. Heidmann et al [1] identify four different flow patterns. At low velocity a closed rim flow pattern was formed. As flow velocity is increased open flow pattern was formed in which rim of one side does not meet the rim of the other side at lower end. At higher velocities periodic drop and fully develop flow patterns were formed. Different flow techniques were used to observe the flow pattern such as flash flow photography and high speed cinematography. Dombrowski and Hooper [2] uses jet velocity and impingement angle to measure the liquid sheet length sheet length and drop size using high speed cinematography. Different flow patterns were formed using laminar and turbulent impinging jets, the flow pattern formed by laminar flow produces smooth and larger sheets as compared to turbulent flow. Anderson [3] also studied the flow spray patterns formed by impinging two turbulent jets. By measuring the sheet breakup length, xb, maximum sheet width W and drop size as a function of flow velocity and injector geometry (2ϕ, d0, L/d0, and lj) Anderson [3] analyzed the spray characteristics of turbulent impinging jets. As liquid impinging jet phenomena is a complex and multiphase flow, limited literature is available for numerical flow simulations addressing dynamics of impinging jet. CIP-LSM (CIP-based level set) and MARS method was used to stimulate the atomization of impinging jets on fixed mesh by Inoue et al[4] in 2008. Considering the fixed mesh, flapping liquid sheet method were observed as the grid was too coarse to accurately resolve the liquid sheet into ligaments and droplets.

The phenomena of liquid impinging jet is divided into two categories: like and unlike-impinging jets. For an unlike-impingement of liquid jets, the fuel and oxidizer jets impinge upon each other in an inclined angle, and the atomization and mixing of propellant takes place simultaneously. For like-impingement, jets with the same liquid impinge with each other and atomization takes place before mixing with similarly atomized particles of other propellant. In this research like-impingement technique was employed.

2 THEORETICAL AND NUMERICAL FRAMEWORK

Equations of fluid flow which are used in this work are impossible to solve analytically i.e. their exact solutions are not available. Numerical methods can be used to solve any differential equation which is otherwise impossible to solve analytically but one major disadvantage of this method is errors associated with it. However these errors can be reduced by employing different techniques. The fluid flow equations used in this research are given below.

International Journal of Scientific & Engineering Research, Volume 12, Issue 11, November-2021
ISSN 2229-5518

2.1 A. Continuity Equation

Continuity equation is a mathematical expression which is based upon the principle of mass conservation which states that mass can neither be created nor be destroyed. By applying the principle of mass conservation to a control volume in a fixed space, continuity equation is obtained in its basic form which is given below

$$\frac{\partial \rho}{\partial t}\iiint \rho \, d\forall + \oiint \rho V.dS = 0$$

Above equation shows the continuity equation in integral form. Continuity equation after some modification in form of Partial Differential Equation is given below:

$$\frac{\partial \rho}{\partial t} + \nabla.(\rho \boldsymbol{u}) = \mathbf{0}$$

$$\rho\left(\frac{\partial \boldsymbol{u}}{\partial t} + \boldsymbol{u}.\nabla \boldsymbol{u}\right) = -\nabla p + \nabla.(2\mu \boldsymbol{D}) + \sigma\kappa\delta_s n$$

Where ρ(x,t) the fluid density, u = (u,v,w) is the velocity vector , D the deformation tensor and μ(x,t) the dynamic viscosity. The radius of curvature of the interface is given by κ and n is defined as unit vector normal to the surface. The Dirac delta function δs shows that the surface-tension co-efficient σ is concentrated on the interface. For the steady flow derivative w.r.t time is zero and above equation can be written as:

$$\nabla.(\rho \boldsymbol{u}) = \mathbf{0}$$

2.2 Momentum Equation

Applying the Newton's second law to a control volume in fixed space gives us the momentum equation. In case of control volume of fluid element the integral form of momentum equation is:

$$\frac{\partial}{\partial t}\iiint \rho V d\forall + \oiint (\rho V.dS)V = -\oiint \rho dS + \iiint \rho f d\forall + F_{viscous}$$

Considering the right side of equation are force terms which include body forces (gravity, electromagnetic etc.) and surface forces (pressure and shear).Momentum equation is partial differential form are given below

$$\frac{\partial(\rho u)}{\partial t} + \nabla.(\rho u V) = -\frac{\partial \rho}{\partial x} + \rho f_x + F_{x_{viscous}}$$

$$\frac{\partial(\rho v)}{\partial t} + \nabla.(\rho v V) = -\frac{\partial \rho}{\partial y} + \rho f_y + F_{y_{viscous}}$$

$$\frac{\partial(\rho w)}{\partial t} + \nabla.(\rho w V) = -\frac{\partial \rho}{\partial z} + \rho f_z + F_{z_{viscous}}$$

Viscous forces on the right side are denoted by Fviscous. When these are replaced by actual viscous term, we get a complete set of equations which are known as Navier Stokes equations.

$$\rho\frac{\partial u}{\partial t} + \rho u\frac{\partial u}{\partial x} + \rho v\frac{\partial u}{\partial y} + \rho w\frac{\partial u}{\partial z}$$

$$= -\frac{\partial \rho}{\partial x} + \frac{\partial}{\partial x}(\lambda\nabla.V + 2\mu\frac{\partial u}{\partial x} + \frac{\partial}{\partial y}\left\{\mu\left(\frac{\partial v}{\partial x} + \frac{\partial u}{\partial y}\right)\right\} + \frac{\partial}{\partial z}\left\{\mu\left(\frac{\partial u}{\partial z} + \frac{\partial w}{\partial x}\right)\right\}$$

2.3 Energy Equation

Energy equation is redundant in the case of incompressible flow where the only unknowns are pressures and velocities which can be obtained from continuity and momentum equations respectively. However, when the flow is compressible there is another unknown which is density and so we need energy equation for that unknown. When applied to a control volume energy equation can be written as:

$$\iiint \dot{q}\,\rho d\forall + \dot{Q_{viscous}} - \oiint \rho V.dS + \iiint \rho(f.V)d\forall + \dot{W_{viscous}}$$

$$= \frac{\partial}{\partial t}\iiint \rho\left(e + \frac{V^2}{2}\right)d\forall + \oiint \rho\left(e + \frac{V^2}{2}\right)V.dS$$

2.4 Volume of Fluid

A variable representing volume fraction of each phase present in the domain is presented using VOF method. Number of variables is equal to the phase count in a domain. Sum of volume fractions of all phases present in a cell is equal to unity. Volume of fluid method is generally used for incompressible fluids (constant density) and thus volume of a phase is also conserved (from conservation of mass). For a fluid named 'q', its volume fraction function is denoted as aq, then this volume fraction function can attain any value based on three different cases represented below:

- aq =0 (No fluid 'q' is present in a cell)
- 0< aq <1 (cell contains some volume of fluid 'q' along with other fluid(s), which means that interface between 'q' fluid and some other fluid(s) is present in this cell)
- aq =1 (cell is entirely filled with fluid 'q')

After assigning the volume fraction function for all phases, continuity equation for each phase is solved to know the location of its interface. For the volume fraction of 'q' fluid in a system containing 'n' number of fluids, continuity equation is given along with the constraint defined for each cell:

$$\sum_{q=1}^{n} \alpha_q = 1$$

$$\frac{\partial \alpha_q}{\partial t} + u_i\frac{\partial \alpha_q}{\partial x_i} = 0$$

International Journal of Scientific & Engineering Research, Volume 12, Issue 11, November-2021
ISSN 2229-5518

Properties such as densities, viscosities etc. in each cell are averaged based on the volume fraction of all fluids and it can be shown as:

$$\rho = \sum p_q \alpha_q$$

Unlike continuity equation, a single momentum equation is solved throughout the domain and solved velocities are shared among all fluids.

3 Geometry Modeling

Geometry of the domain is created using in-built geometry creation tools of ICEM CFD in ANSYS FLUENT. The dimensions of the domain are given below:

Table I. Geometry Dimensions

Impingement Angle	90 Degrees
Injector Diameter	400µm
Computational Domain	50D x30D x10D

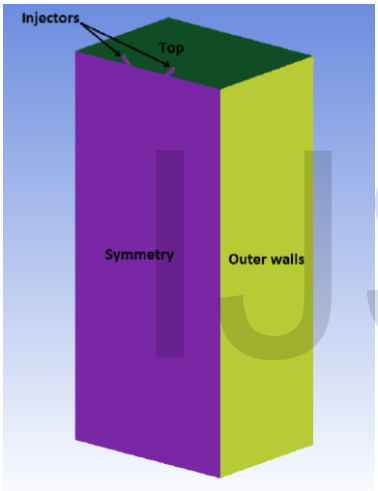

Fig1. Geometry

On top of the cuboid domain, there are two nozzles which are inclined at 45 degrees with respect to the domain and at 90 degrees from each other. The liquid used is a glycerin-water solution and the ambient gas used is air at 298 K temperature and 1atm pressure. In order to neglect the effect of domain boundary, the size of the domain is set to 50D x 30D x 10D. The schematic diagram of flow pattern in case of double liquid impinging jets is given below:

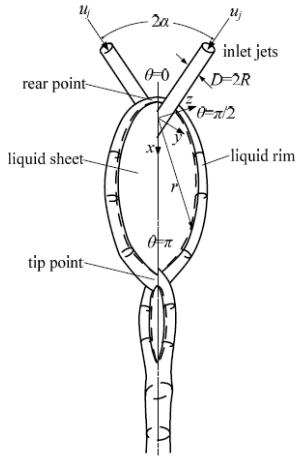

Fig2. Schematic diagram of double impinging jets [5]

4 Grid Generation

Using ANSYS ICEM CFD software structure grid was generated and overall domain is divided into two mesh regions Inner and Outer. Inner region is more refined as compared to outer region because most of the fluid interaction is taken place in that region.

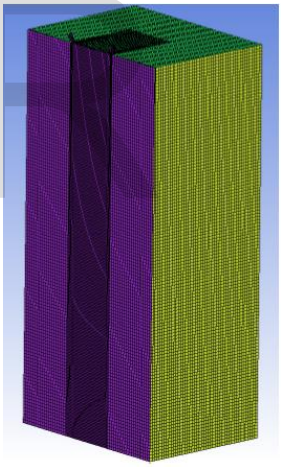

Fig3. Tetrahedral Structured Mesh

5 Adaptive Mesh Refinement

Adaptive mesh refinement is an important tool while carrying out CFD analysis in multiphase flows. With the use of Adaptive Mesh Refinement technique one can define the areas which require more refinement and the areas which require a coarsen mesh depending upon the amount of activity going in that region, all along during the simulation phase. Using the gradient of density method, a refined criteria of 1 and coarse criteria of 0.01 was applied. Which means that mesh will refine in the region which contains density gradient value greater than 1 and mesh will coarsen in the region where density gradient value less than 0.01 exist. Level of refinement means that a selected cell will refine up to that level. If level is 1 than se-

International Journal of Scientific & Engineering Research, Volume 12, Issue 11, November-2021
ISSN 2229-5518

lected cells will be divided into 4 equal cells in 2-D and 8 equal cells in 3-D (for hexahedral cells). If selected level is 2, then these mini cells which were the result of previous one-level refinement will also divide into more cells (if above mentioned criteria is met). So the original cell will divide into 4*4 equal cells in 2-D and 8*8 equal cells in 3-D. In 3rd level of refinement, those cells which were produced from 2nd level of refinement will also refine and so on. Different refinement level are given below:

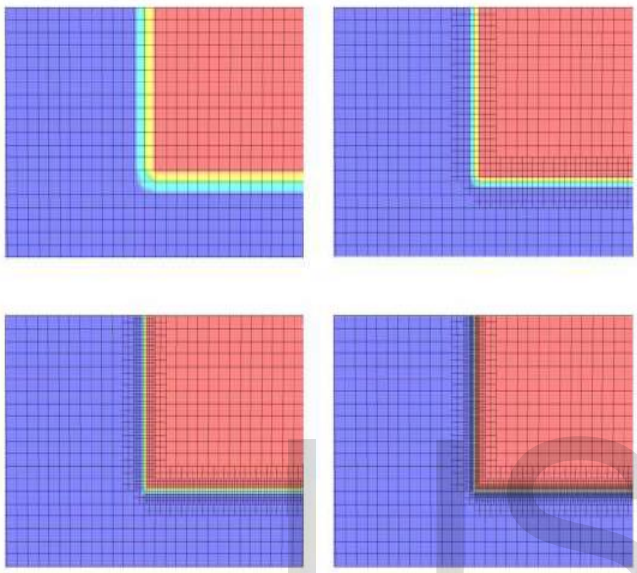

Fig4. Refinement level from 1 to 4

Different refinement level are given below:

Results at different grid refinement level at Vj=3.3 m/s are shown in figure given below. The level-2 shows that fluid sheet have very low thickness and thickness reduces as fluid travels away from the impingement point If at some distance from the impingement point, thickness gets lower than two cell lengths, then this already low thickness gets further dissipated. So at lesser grid refinement levels, fluid sheet cannot be simulated properly. At level-3 and level-4 liquid sheet formed shows a smooth pattern and have close resemblance with the results produced by Vigor Yang [4].

Fig5. Simulation Results at different grid refinement level at Vj=3.3 m/s and D=400µm

6 TIME STEP SIZE

Different refinement level are given below:

Time step size in VOF calculations is usually limited by courant number of the flow. Courant number in a VOF method is a dimensionless number which gives the ratio of time step size used in calculation and time needed for fluid element to pass through one complete control volume. Courant number is limited by the accuracy stability requirements. Usually its value is set to 0.25. From this value and mesh size, we can calculate the time step needed for the calculation.

$$\Delta t = C\frac{\Delta x}{V}$$

7 TURBULENCE MODELING

Different refinement level are given below:

As Reynolds Averaged Navier-Stokes equations were used for simulation so it required some sort of turbulence model to be used. Impinging jets show some sort of turbulence behavior upon impingement which travels downstream in the shape of waves and eventually becomes the reason of liquid ligaments breaking from the main liquid sheet. Liquid sheet thickness prevent the sheet from breaking into ligaments but as the distance from impingement point increases, thickness of the sheet decreases and at one stage it becomes so less to be able to stop ligament formation. Radial velocities of each point in ligaments further plays its role in breaking of ligament into droplets.

As already stated, using laminar flow assumption is not enough to simulate impinging process. As we do not require most accurate solution in terms of turbulence, so we needed a fast and simple model that would do our job just fine. Spalart- Allmaras model was tested from one equation turbulence model category due to its speed but it showed lack of convergence. Next choice in terms of speed were two equation models and thus Standard K-epsilon model was tested. This turbulence model showed good convergence behavior and thus used throughout the simulations.

8 FLOW PATTERNS OF IMPINGING JET

Different refinement level are given below: With the increase in velocity ranging from 2.6m/s to 25m/s various flow patterns were formed which are shown in figure 6. The pattern formed at low velocities was a smooth liquid sheet completely surrounded by liquid rim. As jet velocity is further increased the flow starts to separate at the lower end due to decrease in sheet thickness which results in the formation of ligaments at lower end of sheet. As the liquid sheet becomes unstable, holes are formed which grows progressively, finally reaching the sheet boundary to open the closed rim structure.

First pattern which is formed is a liquid chain, which occurs at velocity 2.6m/s. With further increase in velocity to 3.3m/s a closed rim type pattern was observed in which rim of both sides meet at the lower end. As the velocities is further increased to 7.2 m/s, the length and width of the liquid sheet starts to increase which results in decrease of sheet thickness.

International Journal of Scientific & Engineering Research, Volume 12, Issue 11, November-2021
ISSN 2229-5518

The sheet starts to break at the lower end of the sheet and open rim flow pattern is obtained. With further increase in velocity from 7.2m/s disturbance starts to initiate at the impinging point and grow, while circulating downstream along the liquid rim. Due to the influence of inertial forces the liquid sheet reaches to its minimum thickness value. As sheet thickness is reduced, surface tension forces overcome the inertial forces and sheet break into ligaments. The ligaments are further converted into droplets and the pattern is called fully developed flow as define by Vigor Yang [4].

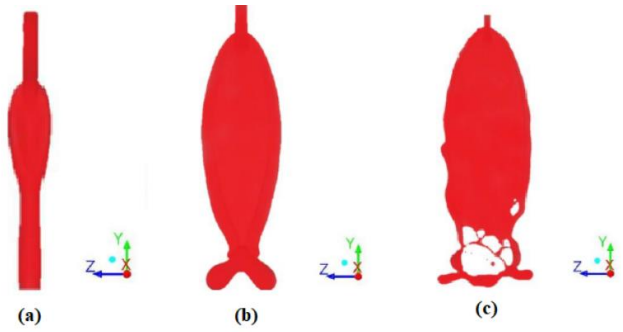

Fig6-1. Impinging Jet flow patterns of Glycerin-Water Solution9 (a) Liquid Chain (u_j=2.6m/s) (b) Closed Rim (u_j=3.3m/s) (c) Open Rim (u_j=7.2m/s)

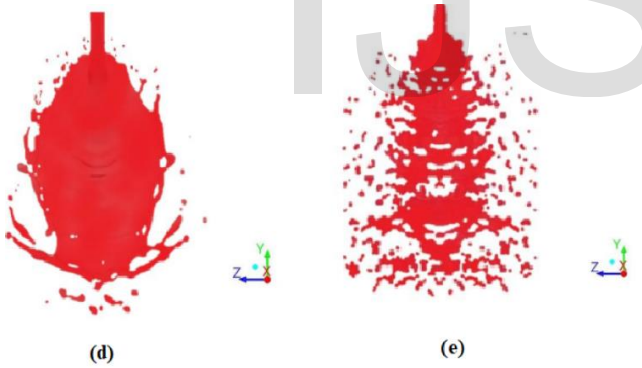

Fig6-1. Impinging Jet flow patterns of Glycerin-Water Solution9 (d) Unstable Rim (u_j=16m/s) (b) Fully Develop flow (u_j= 25 m/s)

9 Liquid Sheet Characteristics

The droplet data is calculated by using User Defined Function (UDF) present in ANSYS FLUENT. The Sauter mean diameter D[3,2] is calculated at velocities of 7.2 m/s ,16 m/s and 25 m/s. The results obtained are related with the experimental results of Lai[5].

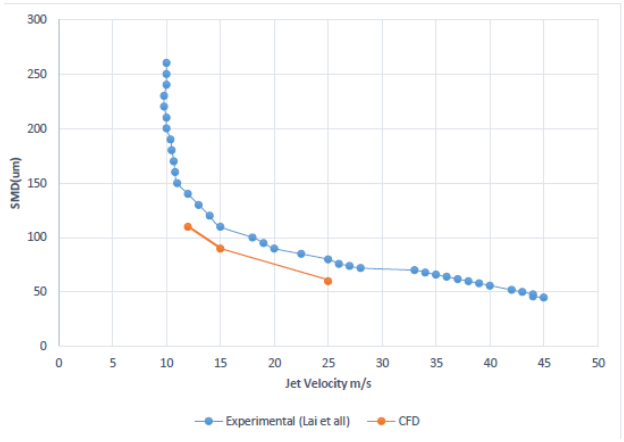

Fig7. Comparison of SMD w.r.t Jet Velocity

The CFD results have lesser SMD than experimental results. The main reasons for the difference are:

- Lai[5] uses Water as fluid whereas in this study Glycerin-Water solution is used , which is more viscous than water.
- Experimental results will be collected at some point downstream of the impingement point. In case of Lai, the results are collected at 10mm downstream of the impingement point. While considering the CFD result, they diameter of droplets are collected for whole region.
- While using the UDF Fluent technique, all diameters greater than 400µm are ruled out because they are to convert into droplets. But in case experimental studies this ruling probably not been carried out.

Different refinement level are given below: Maximum Liquid Sheet Width and Length for Velocities 2.6m/s, 3.3m/s and 7.6m/s were compared with the experimental results obtained by Heidmann[1]. It was found that with the increase in jet velocity length and width of liquid sheet tend to increase until a point it is converted into ligaments and finally into droplets

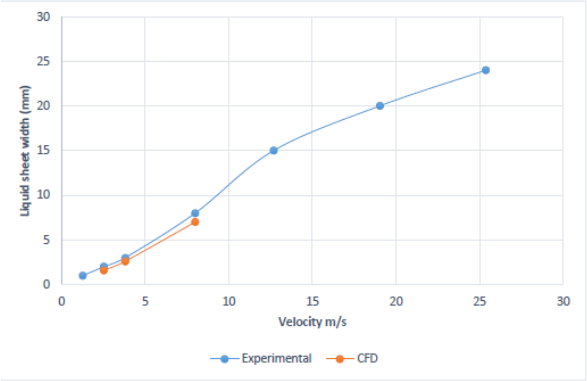

Fig8. Max Liquid Sheet Width w.r.t Jet Velocity

International Journal of Scientific & Engineering Research, Volume 12, Issue 11, November-2021
ISSN 2229-5518

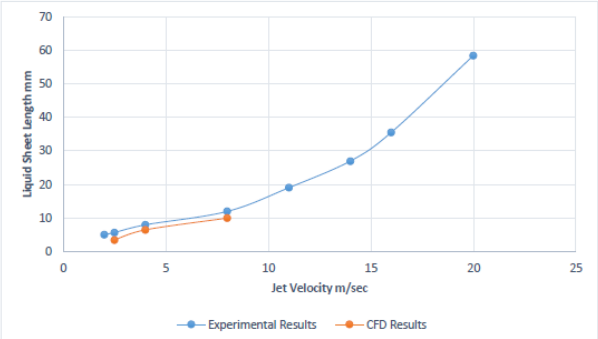

Fig9. Max Liquid Sheet Length w.r.t Jet Velocity

Droplet velocities are plotted taken into account of vertical axis from the point of impingement. Angles are also measured with respect to vertical axis. The result are related with the results obtained by Lai et al[5]. The experimental results obtained by Lai are compared with the CFD results obtained at velocity 25m/s. The results are non-dimensionlaized by dividing the shedding drops velocities by jet velocity. General trend of the velocities are shown below

Fig10. Comparison of shedding drops velocities along Vertical Axis

10 CONCLUSIONS

In this research liquid impinging jet phenomena is simulated using Volume of Fluid (VOF) method of ANSYS FLUENT 16.0. Glycerin-Water Solution was used as fluid and the results obtained are related with the already present experimental results. During the simulation phase with increasing velocity of jet fluid, different flow patterns were obtained. At low speed closed rim pattern was obtained in which rim of both sides meet at the lower end and a smooth pattern is obtained. With the increase in velocity the length and width of the liquid sheet tends to increase but at the dispense of liquid sheet thickness, which starts to decrease at the lower end and open rim flow pattern is obtained. In case of open rim pattern rim of both side does not meet at the lower end and results in the formation of ligaments.

It was found that the results accuracy was extremely dependent on grid refinement. But with the increase in grid refinement it's become more and more difficult to get a converge solution. The main reason is the use of Courant Number in VOF method. With the increase in refinement courant number also increases, but to keep Courant number in stable limits time step size is required to increase with increasing velocity which results in additional computational power and time.

When fluid ligaments are finally break down into ligaments, the droplets formed does not change their shape so much after that. The main reason is that the droplets starts to move away from the impinging point and after large number of time step they try to cover the whole domain. As droplets cover the whole domain, refinement of whole domain is required which increases the domain size to a very high value and if AMR refinement refinement technique is applied, its starts to fail. To solve this problem domain geometry size can be reduced but it will affect the results due to boundary conditions.

REFERENCES

[1]R. J. P. Marcus F. Heidmann, Jack C. Humphrey, "A study of sprays formed by two impinging jets," NACA Technical Note 3835, 1957.

[2]N. a. H. Dombrowski, "A study of the spray formed by impinging jets in laminar and turbulent flow," Journal of Fluid Mechanics, 1964.

[3]H. W. E. Anderson, M, Ryan, S. Pal, and R, J. Santoro, "Fundamental Studies of Impinging Liquid Jets," AlAA 92-0458, 1992.

[4]X. C. Vigor Yang, Dongjun Ma, & Stephane Popinet, "High-fidelity simulations of impinging jet atomization," Atomization and Sprays, vol. 23, 2013.

[5]W. H. a. T. L. J. W. H. Lai, "Effects of Orifice Size and Impinging Angle on the Characteristics of a Like-Doublet Impinging-Jet," International Journal of Turbo and Jet Engines, 1998.

[6]R. J. P. Marcus F. Heidmann, Jack C. Humphrey, "A study of sprays formed by two impinging jets," NACA Technical Note 3835, 1957.

[7]R. H. Anderson WE, Santoro RJ, "Impact wave-based model of impinging jet atomization." Atomization and Sprays, 2006.

[8]E. A. Ibrahim, "Comment on "Atomization Characteristics of Impinging Liquid Jets"," Journal Of Propulsion And Power, 2009..

[9]A. P. Hasson, R. E., "Thickness Distribution in a Sheet Formed by Impinging Jets," AIChE Journal, 1964

[10]J. H. Ferziger, Peric, Computational Methods For Fluid Dynamics, 3rd reviewed edn ed.: Springer-Verlag, 2002.

[11]C. W. Hirt, Nichols, B. D., "Volume of fluid (VOF) method for the dynamics of free boundaries," Journal of Computational Physics, vol. 39, pp. 201–255, 1981.

[12]D. L. Youngs., "Time-Dependent Multi-Material Flow with Large Fluid Distortion," in Numerical Methods for Fluid Dynamics, K. W. M. a. M. J. Baines, Ed., ed: Academic Press, 1982.

[13] O. Ubbink, "Numerical prediction of two fluid systems with sharp interfaces," PhD, Imperial College, London, 1997